Local thermal resonance control of GaInP photonic crystal membrane cavities using ambient gas cooling

Sergei Sokolov, Jin Lian, Emre Yüce, Sylvain Combrié, Gaelle Lehoucq, Alfredo De Rossi, and Allard P. Mosk

---

Articles you may be interested in

Quasiresonant excitation of InP/InGaP quantum dots using second harmonic generated in a photonic crystal cavity
Appl. Phys. Lett. **101**, 161116 (2012); 10.1063/1.4761248

Control of spontaneous emission from InP single quantum dots in GaInP photonic crystal nanocavities
Appl. Phys. Lett. **97**, 181104 (2010); 10.1063/1.3510469

Electrically injected InGaAs/GaAs photonic crystal membrane light emitting microcavity with spatially localized gain
J. Appl. Phys. **104**, 123103 (2008); 10.1063/1.3040690

Efficient coupling to W1 photonic crystal waveguide on InP membrane through suspended access guides
Appl. Phys. Lett. **92**, 061105 (2008); 10.1063/1.2841817

Two-dimensional Al Ga In P∕Ga In P photonic crystal membrane lasers operating in the visible regime at room temperature
Appl. Phys. Lett. **90**, 011113 (2007); 10.1063/1.2430488

Local thermal resonance control of GaInP photonic crystal membrane cavities using ambient gas cooling

Sergei Sokolov,[1,a] Jin Lian,[1] Emre Yüce,[1] Sylvain Combrié,[2] Gaelle Lehoucq,[2] Alfredo De Rossi,[2] and Allard P. Mosk[1]

[1]*Complex Photonic Systems (COPS), MESA+ Institute for Nanotechnology, University of Twente, 7500 AE Enschede, The Netherlands*
[2]*Thales Research & Technology, Route Départementale 128, 91767 Palaiseau, France*

We perform spatially dependent tuning of a GaInP photonic crystal cavity using a continuous wave violet laser. Local tuning is obtained by laser heating of the photonic crystal membrane. The cavity resonance shift is measured for different pump positions and for two ambient gases: He and N_2. We find that the width of the temperature profile induced in the membrane depends strongly on the thermal conductivity of the ambient gas. For He gas, a narrow spatial width of the temperature profile of 2.8 μm is predicted and verified in experiment. © 2015 AIP Publishing LLC.
[http://dx.doi.org/10.1063/1.4919386]

Photonic crystal (PhC) cavities are widely studied because of their fascinating applications.[1–3] Arrays of PhC cavities can form coupled resonator optical waveguides (CROWs), which are very promising for slow light applications[4] and the study of light localization.[5] Various fabrication imperfections can cause a disorder in a CROW structure which leads to a detuning of cavities from the intended resonance and reduces the waveguide throughput and bandwidth. Tuning each cavity independently can restore cavities in resonance and counteract the disorder. There is a variety of methods to change the refractive index of a PhC cavity, including free-carrier injection,[6] the nonlinear Kerr effect,[7] thermal effects,[8,9] oxidation,[10–12] and chemical processes.[13] Of these methods, thermal tuning through local laser heating is easy, reversible, and can give a steady-state control of the resonance properties of the system. However, due to the diffusion of heat in the PhC membrane, thermal control of one cavity will affect the neighbor cavities. The width of the temperature profile is determined by the sample material and the surrounding media. Therefore, one can expect that by carefully selecting the sample material and ambient medium one can control the width of the temperature profile.

In this work, we use the semiconductor alloy $Ga_{0.51}In_{0.49}P$ as a sample material and two gases, nitrogen and helium, as surrounding media. $Ga_{0.51}In_{0.49}P$ has a thermal conductivity[14] of 4.9 W/(m·K), which is quite small in comparison with other semiconductor materials.[15] The thermal conductivity of gases is often assumed to be negligible compared to semiconductors such as Si. However, the effect of the gas on the width of the thermal profile depends strongly on the ratio of the thermal conductivity of the gas and the semiconductor. Helium has a high thermal conductivity[16] of 0.153 W/(m·K), which is more than 6 times higher than of nitrogen[16] (0.024 W/(m·K)) and only 32 times smaller that that of $Ga_{0.51}In_{0.49}P$. Therefore, the combination of $Ga_{0.51}In_{0.49}P$ and He should have a high thermal exchange efficiency and small width of the temperature profile in

comparison with other materials. To investigate the width of the temperature profile in PhC membranes, we measured the response of the resonance of a H0-type cavity to a spatially scanned continuous wave (CW) heating laser focused on the membrane.

The PhC H0 nanocavity is implemented in a triangular lattice of air holes with a period $a = 505$ nm and a hole radius 0.24 a. The hole shift for the H0 cavity is 0.16 a. A subharmonic hole structure is induced to enhance the radiation from the cavity in a vertical direction.[17] The cavity is made of a suspended membrane of $Ga_{0.51}In_{0.49}P$ with a thickness of 180 nm. The membrane is covered with 30 nm of Si_3N_4 on the top using a PECVD technique to tune the cavity resonance. The detailed description of the fabrication method can be found in Ref. 18. A microscope picture of the cavity with the surrounding PhC is presented in Fig. 1(a). The cavity is close to the center of the membrane and the IR light is evanescently coupled through a PhC waveguide. Mode converters at the end of the waveguide decrease the Fabry-Perot interference in the waveguide and increase the coupling efficiency.[19]

The setup is shown in Fig. 1(b). The CW IR laser probe light was coupled to the PhC waveguide using a polarization maintaining lensed fiber with NA of 0.55. The out-of-plane scattered light was collected using a 0.4 NA objective and imaged on an IR CCD camera using tube lens L2. The total magnification of the system is 50×. We recorded spectra by sweeping the wavelength of the IR laser and taking IR
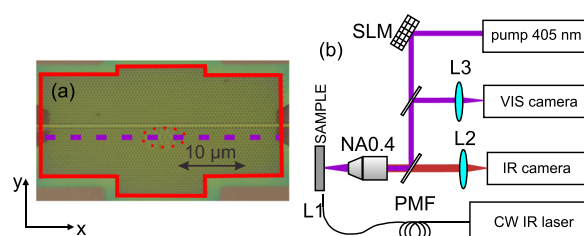

FIG. 1. (a) Optical microscope image of a GaInP PhC (red line) with an H0 cavity (red dotted ellipse) in the center. (b) The pump-probe setup.

a)s.sokolov@utwente.nl. URL: http://cops.nano-cops.com

camera snapshots for each wavelength. The oxygen concentration was reduced to less than 0.025% to suppress oxidation effects.[10–12] The chamber was kept at a slight overpressure (less than 2 mbar above atmospheric pressure). Thermal tuning was performed using a 405 nm CW diode laser, which was focused onto the surface of the sample into a spot with a FWHM of 0.96 μm using the same objective. The surface of the sample with the pump spot was also imaged with a visible range camera using tube lens L3 with a system magnification of 27×. The position of the pump spot was controlled using a spatial light modulator. The pump spot was moved along a line through the center of the cavity (see Fig. 1(a)) and the resonance spectrum of the cavity was measured for a sequence of pump positions. Any effects of slow oxidation or water coverage are eliminated by alternating between reference spectra (without pump laser) and signal spectra (with pump).

Resonance spectra for the reference and for pump positions of 0 and 5 μm relative to the center of the cavity in N_2 are presented in Fig. 2. The closer the pump spot is placed to the cavity, the stronger the redshift is due to the better overlap of the temperature profile and the cavity mode. We observe two resonance modes: the high-Q low-frequency mode (M1) and the low-Q high-frequency M2. Both resonances have a distinct Lorentzian shape and quality factors of about 1000 and 300 are estimated for modes M1 and M2, respectively. The calculated loaded Q-factor of the mode M1 is about 2500, because the cavity is designed to be overcoupled. The resonance M2 corresponds to a higher order mode which is predicted from calculations. The mode M1 is much brighter than M2. The two modes have slightly different spatial positions, and the reference position is the center of mode M1. We use the wavelength shift of mode M1 to determine the spatially dependent cavity response to the pump. Apart from the redshift, we observed a reduction of the intensity of the out-of-plane scattered light when the pump was positioned close to the cavity. We attribute this reduction to the fact that the cavity resonance was tuned farther away from the PhC band, thereby reducing the evanescent coupling to the waveguide.

The pump power incident on the sample was 110 μW in N_2 atmosphere. The spatial response curve for N_2
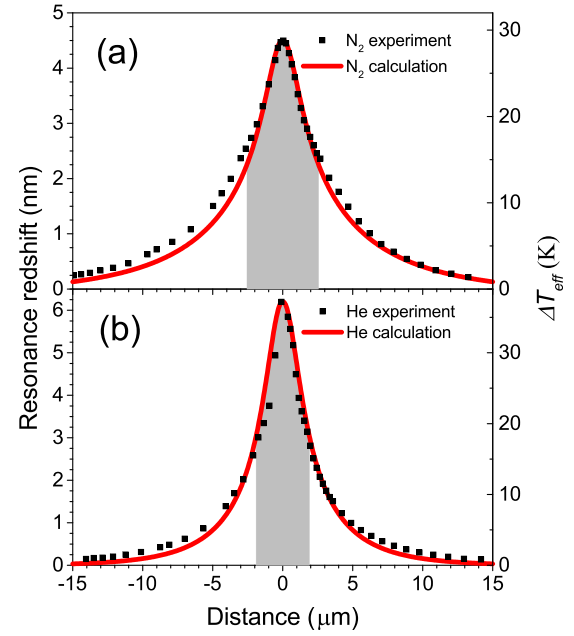
FIG. 3. Redshift of the cavity resonance and ΔT_{eff} for different pump positions with nitrogen (a) and helium (b) as an ambient gas. Red curves represent the redshift calculated according to the model. From one measurement to another, we observed an error less than 3% of the shift for N_2, and less than 1% for He.

atmosphere is presented in Fig. 3(a). The maximum redshift is 4.5 nm and the FWHM spatial width (Δx_{eff}) of the tuning curve is 5.1 μm. In He atmosphere, a larger pump power of 220 μW was used (see Fig. 3(b)). The maximum observed redshift is 6.2 nm and Δx_{eff} is only 3.7 μm. As a result of the high thermal conductivity of the He, both the redshift (normalized to power) and Δx_{eff} are smaller by 30% compared to N_2. This thermal profile can be used to predict thermal crosstalk in structures with multiple cavities such as CROWs. Compensation of crosstalk is typically possible when the crosstalk is below about 50%, i.e., for elements spaced more than $\Delta x_{eff}/2$. A reduction of Δx_{eff} therefore directly translates into a higher possible integration density of independently tuned cavities.

We have performed numerical calculations to model the resonance wavelength change of the cavity for different pump positions taking into account material and pump properties. For small perturbations of the refractive index, the wavelength change can be expressed as[20]

$$\Delta \lambda = \frac{\lambda}{\langle n \rangle} \frac{dn}{dT} \Delta T_{eff}, \tag{1}$$

with

$$\Delta T_{eff} = \frac{\int \Delta T(\mathbf{r} - \mathbf{r}_0) \epsilon(\mathbf{r}) |\mathbf{E}(\mathbf{r})|^2 d^3 r}{\int \epsilon(\mathbf{r}) |\mathbf{E}(\mathbf{r})|^2 d^3 r}, \tag{2}$$

where ΔT_{eff} is temperature averaged over the mode profile $\epsilon(\mathbf{r}) |\mathbf{E}(\mathbf{r})|^2$ of the cavity, $\epsilon(\mathbf{r})$ is the dielectric constant of the membrane material, $\Delta T = T - T_0$ is the local temperature change in the PhC averaged over the membrane thickness, $\frac{dn}{dT}$ is the linear coefficient of the refractive index temperature response, $\langle n \rangle$ is the averaged refractive index of the
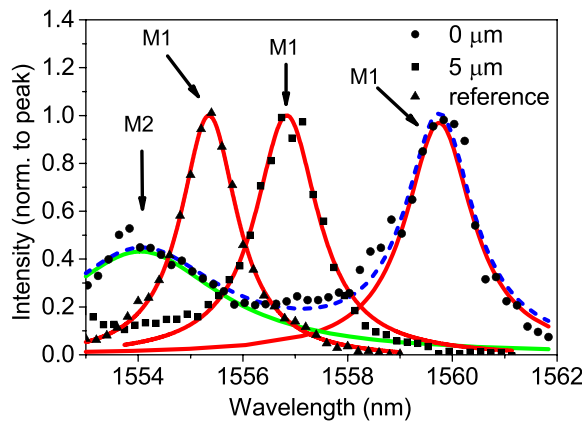
FIG. 2. Spectra obtained from the out-of-plane scattered light for no-pump reference and for pump positions on top of the cavity and 5 μm away from the center of the cavity in N_2 atmosphere. Color lines are Lorentzian fits.

membrane material, and $\mathbf{r}_0$ is the position of the pump. $T_0 = 293.15$K is the ambient temperature. The mode profile was calculated using a finite difference time domain method.[21] Temperature profiles were calculated in COMSOL using a steady state heat diffusion model with a constant source term assuming that thermal conductivities are not temperature dependent within the relevant temperature range

$$\kappa(x, y, z)\nabla^2 T(x, y, z) + W(x, y, z) = 0, \qquad (3)$$

where $\kappa(x, y, z)$ is the thermal conductivity and W is a source term inside the membrane written as a sum of two terms $W = W_E + W_R$, due to the excess energy of the carriers and their recombination, respectively.

We observe photoluminescence (PL) of $Ga_{0.51}In_{0.49}P$ at 670 nm caused by the pump light. The bandgap of $Ga_{0.51}In_{0.49}P$ is 1.85 eV and the energy of a 405 nm photon is 3.06 eV. The excess energy term (W_E) is released within about a picosecond upon optical excitation and therefore has the spatial profile of the pump spot (a Gaussian width $\sigma_E = 0.41\ \mu m$) and corresponds to a fraction $f_E = 0.4$ of the initial power. The recombination term (W_R) has the profile of the PL spot, a Gaussian width $\sigma_R = 0.50\ \mu m$, and it takes a fraction $f_R = 0.6$ of the photon energy. We assume that all absorbed light is converted into heat, because the estimated radiative carrier recombination efficiency is less than 1%. The excess energy term is expressed as

$$W_E(x, y, z) = f_E \frac{P(1 - R)}{2\pi\sigma_E^2} \alpha e^{-(x^2+y^2)/2\sigma_E^2} e^{-\alpha z}. \qquad (4)$$

Here, R is the reflection coefficient of the membrane estimated to be 9.5%, α is the absorption coefficient of $Ga_{0.51}In_{0.49}P$, and P is the total power of the pump beam. The recombination heating term has the same Gaussian shape with the appropriate fraction and width inserted. The size of the air gap between the membrane and GaAs substrate for our samples is equal to 1.5 μm, the size of the air layer above the membrane was taken to be 10 μm. All external boundaries are Dirichlet type with temperature T_0. The photonic crystal is assumed to be a rectangle of $40 \times 20\ \mu m$. Dirichlet boundaries are considered because the membrane is surrounded from four sides by the bulk material, which acts like a perfect heat sink. Thermal conductivities for gases were taken from Ref. 16. The coating layer made of Si_3N_4 has a thermal conductivity[22] of 24.5 W/(m·K). The thermal conductivity of the membrane was taken as volume averaged between holes of the PhC lattice and two layers of Si_3N_4 and $Ga_{0.51}In_{0.49}P$. The absorption coefficient[23] of $Ga_{0.51}In_{0.49}P$ at 405 nm is 24.5 $(\mu m)^{-1}$ and the absorption coefficient[24] of Si_3N_4 is less than 0.006 $(\mu m)^{-1}$. As a result nearly all pump light is absorbed by the $Ga_{0.51}In_{0.49}P$ membrane. The temperature profile can be calculated without any free parameters. The only parameter which is unknown for the redshift calculation is $\frac{dn}{dT}$ for $Ga_{0.51}In_{0.49}P$.

The resulting effective temperature profiles are presented in Figs. 3(a) and 3(b) and are in excellent agreement with the experiment for both nitrogen and helium. The maximum temperature rise in case of nitrogen atmosphere is 29 K, and in case of He it is 37 K, so the ratio of these two
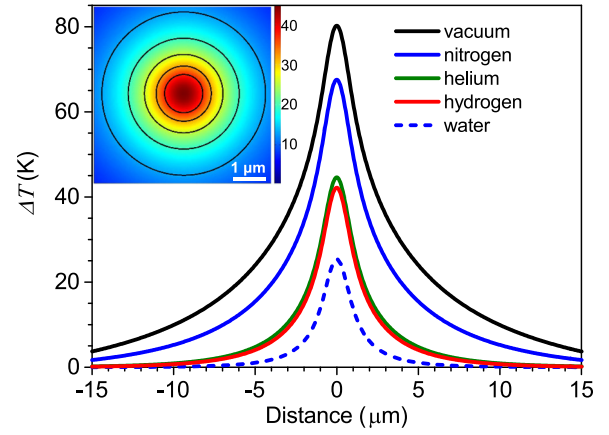

FIG. 4. X-axis cross section of the calculated temperature profile (ΔT) for different ambient media. The pump focus is placed in the center of the cavity. The power of the pump light is 220 μW. The inset shows the 2D averaged temperature profile for helium. The isotherms have a step of 6.3 K.

values normalized to the incident power is equal to 0.63. The experimental ratio of redshifts is 0.69. From Fig. 3, we also estimate the so far unknown $\frac{dn}{dT}$ for $Ga_{0.51}In_{0.49}P$. We obtain the value of $3.1 \pm 0.5 \times 10^{-4}\ K^{-1}$.

Instead of helium, one could use media with a higher thermal conductivity. In Fig. 4, calculated temperature profiles along the central line of the PhC membrane (see Fig. 1) are presented for different surrounding media. These are bare temperature profiles, not convolved with the cavity mode. The widest temperature profile is found in case of vacuum. Water has a thermal conductivity 4 times higher than He, which results in a significantly narrower temperature profile. We note that low-refractive-index liquids such as acetone and isopropanol have thermal conductivities comparable to that of He. Using liquids for heat exchange completely changes the optical properties of the sample, therefore, using a high-thermal-conductivity gas is a more appropriate option in many cases.
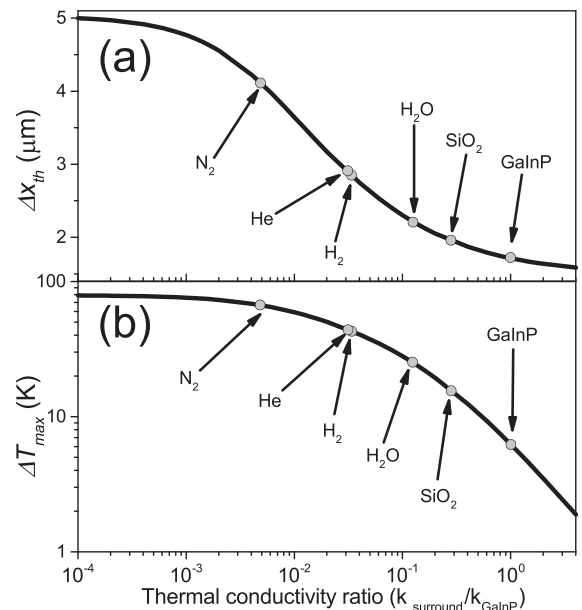

FIG. 5. Calculated Δx_{th} (a) and ΔT_{max} (b) vs thermal conductivity ratio of surrounding media and $Ga_{0.51}In_{0.49}P$. Some well-known materials are marked. The power of the pump light is 220 μW.

The general tendency of the width Δx_{th} and the peak value (ΔT_{max}) of the bare temperature profile is presented in Fig. 5. In case of low ambient thermal conductivity heat tends to diffuse inside the membrane, therefore, Δx_{th} and the peak temperature reach constant values of 5 μm and 79 K, respectively. For large thermal conductivities of the surrounding media, all heat diffuses rapidly into the ambient media reducing Δx_{th} and the peak temperature.

Gas cooling is most relevant for thermal tuning of resonances in membranes made of materials with small thermal conductivities such as $Ga_{0.51}In_{0.49}P$. In highly conducting materials like Si, the thermal profile is significantly larger[9] and is typically determined by the material boundaries rather than by heat exchange with the gas.

For time-dependent tuning applications such as a switch or a tracking filter, the time response is of importance. From time-dependent simulations, we estimate that the 10%–90% temperature rise time in a nitrogen atmosphere is about 6 μs, but in helium it reduces to 2 μs. Therefore, helium not only helps to improve the spatial resolution of thermal tuning but also makes the tuning response about three times faster. Similarly, it should reduce thermal optical nonlinearities that result from absorption of cavity-enhanced probe light.

In conclusion, we measured the spectral tuning curve of a thermally tuned cavity for different surrounding media and found an excellent agreement between experiment and our numerical calculations. Our results and our calculations are of importance for applications such as thermal control of CROWs where the width of the temperature profile should be minimized. Also our calculations offer insight in the role of ambient materials for any applications that involve local laser heating.

[1]A. Yariv, Y. Xu, R. K. Lee, and A. Scherer, Opt. Lett. **24**, 711 (1999).
[2]Y. Akahane, T. Asano, B. Song, and S. Noda, Nature **425**, 944 (2003).
[3]A. B. Matsko, *Practical Applications of Microresonators in Optics and Photonics* (CRC Press, 2009).
[4]N. Matsuda, E. Kuramochi, H. Takesue, and M. Notomi, Opt. Lett. **39**, 2290 (2014).
[5]S. Mookherjea, J. S. Park, S. Yang, and P. R. Bandaru, Nat. Photonics **2**, 90 (2008).
[6]C. Husko, A. De Rossi, S. Combrié, Q. V. Tran, F. Raineri, and C. W. Wong, Appl. Phys. Lett. **94**, 021111 (2009).
[7]E. Yüce, G. Ctistis, J. Claudon, E. Dupuy, R. D. Buijs, B. de Ronde, A. P. Mosk, J.-M. Gérard, and W. L. Vos, Opt. Lett. **38**, 374 (2013).
[8]M. Notomi, A. Shinya, S. Mitsugi, G. Kira, E. Kuramochi, and T. Tanabe, Opt. Express **13**, 2678 (2005).
[9]J. Pan, Y. Huo, K. Yamanaka, S. Sandhu, L. S. R. Timp, M. L. Povinelli, S. Fan, M. M. Fejer, and J. S. Harris, Appl. Phys. Lett. **92**, 103114 (2008).
[10]C. J. Chen, J. Zheng, T. Gu, J. F. McMillan, M. Yu, G. Lo, D. Kwong, and C. W. Wong, Opt. Express **19**, 12480 (2011).
[11]H. S. Lee, S. Kiravittaya, S. Kumar, J. D. Plumhof, L. Balet, L. H. Li, M. Francardi, A. Gerardino, A. Fiore, A. Rastelli, and O. G. Schmidt, Appl. Phys. Lett. **95**, 191109 (2009).
[12]F. Riboli, N. Caselli, S. Vignolini, F. Intonti, K. Vynck, P. Barthelemy, A. Gerardino, L. Balet, L. Li, A. Fiore, M. Gurioli, and D. Wiersma, Nat. Mater. **13**, 720 (2014).
[13]K. Hennessy, A. Badolato, A. Tamboli, P. M. Petroff, E. Hu, M. Atature, J. Dreiser, and A. Imamoglu, Appl. Phys. Lett. **87**, 021108 (2005).
[14]S. Adachi, J. Appl. Phys. **102**, 063502 (2007).
[15]M. Levinshtein, S. Rumyantsev, and M. Shur, *Handbook Series on Semiconductor Parameters* (World Scientific, 1996), Vol. 1.
[16]H. Anderson, *A Physicist's Desk Reference* (American Institute of Physics, NY, 1989).
[17]N. Tran, S. Combrié, P. Colman, A. De Rossi, and T. Mei, Phys. Rev. B **82**, 075120 (2010).
[18]S. Combrié, S. Bansropun, M. Lecomte, O. Parillaud, S. Cassette, H. Benisty, and J. Nagle, J. Vac. Sci. Technol. B **23**, 1521 (2005).
[19]Q. Tran, S. Combrié, P. Colman, and A. De Rossi, Appl. Phys. Lett. **95**, 061105 (2009).
[20]J. Joannopoulos, S. G. Johnson, J. N. Winn, and R. D. Meade, *Photonic Crystals Molding the Flow of Light* (Princeton University Press, 2008).
[21]A. F. Oskooi, D. Roundy, M. Ibanescu, P. Bermel, J. D. Joannopoulos, and S. G. Johnson, Comput. Phys. Commun. **181**, 687 (2010).
[22]See http://www.mit.edu/~6.777/matprops/matprops.htm for MIT material property database.
[23]M. Schubert, V. Gottschalch, C. M. Herzinger, H. Yao, and P. G. Snyder, J. Appl. Phys. **77**, 3416 (1995).
[24]E. Palik, *Handbook of Optical Constants of Solids* (Academic Press, 1985).